International Journal of Computer Vision 23(2), 115–129 (1997)

Following Cusps

ROBERTO CIPOLLA
Department of Engineering, University of Cambridge, Trumpington Street, Cambridge CB2 1PZ, England
cipolla@eng.cam.ac.uk

GORDON FLETCHER AND PETER GIBLIN
Department of Pure Mathematics, The University of Liverpool, P.O. Box 147, Liverpool L69 3BX, England
gordon@liv.ac.uk
pjgiblin@liv.ac.uk

Received October 4, 1994; Revised March 2, 1995; Accepted September 10, 1995

Abstract. It is known that the deformation of the apparent contours of a surface under perspective projection and viewer motion enable the recovery of the geometry of the surface, for example by utilising the *epipolar parametrization*. These methods break down with apparent contours that are singular i.e., with *cusps*. In this paper we study this situation and show how, nevertheless, the surface geometry (including the Gauss curvature and mean curvature of the surface) can be recovered by *following the cusps*. Indeed the formulae are much simpler in this case and require lower spatio-temporal derivatives than in the general case of nonsingular apparent contours. We also show that following cusps does not by itself provide us with information on viewer motion.

1. Introduction

For smooth curved surfaces an important image feature is the profile or apparent contour. This is the projection of the locus of points on the surface which separates the visible and occluded parts. See Fig. 1. Under perspective projection this locus—the critical set or contour generator—can be constructed as the set of points on the surface which are touched by rays through the projection centre. The contour generator is dependent on the local surface geometry (via tangency and conjugacy constraints) and the viewpoint. Each viewpont will generate a different contour generator with the contour generators 'slipping' over the visible surface under viewer motion.

The family of contour generators generated under continuous viewer motion can be used to represent the visible surface. Giblin and Weiss (1987) and Cipolla and Blake (1992) have shown how the spatio-temporal analysis of deforming image apparent contours (*profiles*) enables computation of local surface curvature along the corresponding contour generator (*critical sets*) on the surface, assuming viewer motion is known. To perform the analysis, however, a spatio-temporal parametrization of image-curve motion is needed, but is underconstrained. The *epipolar* parametrization is most naturally matched to the recovery of surface curvature. In this parametrization (for both the spatio-temporal image and the surface), *correspondence* between points on successive snapshots of an apparent contour is set up by matching along epipolar lines. Namely the corresponding ray in the next viewpoint (in an infinitesimal sense), is chosen so that it lies in the epipolar plane defined by the viewer's translational motion and the ray in the first viewpoint. The parametrization leads to simplified expressions for the recovery of depth and surface curvature from image velocities and accelerations and known viewer motion. It is especially suited to the recovery of surface geometry by an active explorer making deliberate viewer motions around an object of interest and it has been successfully implemented in various systems

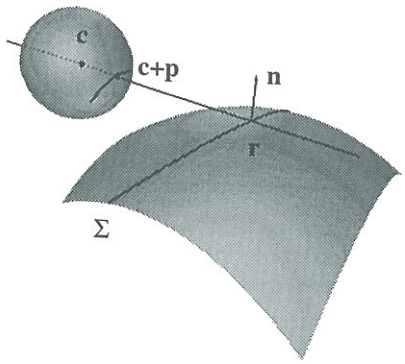

Figure 1. Perspective projection: the contour generator Σ with a typical point $\mathbf{r}$, the image sphere with centre $\mathbf{c}$ and the corresponding apparent contour point $\mathbf{c} + \mathbf{p}$. Thus $\mathbf{p}$ is the unit vector joining the centre $\mathbf{c}$ to the apparent contour point.

(Cipolla and Blake, 1992; Vaillant and Faugeras, 1992).

There are however several cases in which this parametrization is degenerate and so can not be used to recover the local surface geometry. The first case of degeneracy occurs when the contour generator does not *slip* over the surface with viewer motion but is fixed to it. This is the case of viewing a 3D rigid curve attached to the surface such as a surface marking. In this case the epipolar parametrization successfully allows the recovery of the structure of a space curve from image velocities (it is analogous to stereo reconstruction in the infinitesimal limit) but the surface orientation is no longer completely defined but constrained to be perpendicular to the curve tangent. This case poses no special problems. In fact one advantage of the epipolar parametrization is that it leads to a uniform treatment to the recovery of depth for rigid space curves as well as the occluding contours of smooth surfaces. The former can be simply treated as occluding contours with infinite curvature in the direction of the viewing ray—a property which has been successfully used to discriminate between fixed space curves and the occluding contours of smooth surfaces.

Another case of degeneracy occurs at a point of the surface-to-image mapping when a ray is tangent not only to the surface but also to the contour generator. This will occur when viewing a hyperbolic surface patch along an asymptotic direction. For a transparent surface this special point on the contour generator will appear as a *cusp* on the apparent contour. For opaque surfaces, however, only one branch of the cusp is visible and the contour ends abruptly (Koenderink and Van Doorn, 1982; Koenderink, 1984). We call such a surface point a *cusp generator point* and the corresponding image point simply a *cusp point*. See Fig. 2.

The epipolar parametrization of the surface will be degenerate at these cusp generator points since the ray and contour generator are parallel and do not form a basis for the tangent plane. The epipolar spatio-temporal parametrization under viewer motion of the apparent contours can no longer be used to recover depth, surface orientation and surface curvature at these points. Under viewer motion the locus of the cusp generator points on the surface defines the *cusp generator curve*. In the vicinity of this surface strip the epipolar parametrization will be ill-conditioned and impractical.

The remaining cases of degeneracy of the epipolar parametrization will not concern us here—they come from singular contour generators ('lips/beaks' transitions) and frontier points (where the epipolar plane is tangent to the surface). See (Giblin and Weiss, 1995; Giblin et al., 1994) for further details.

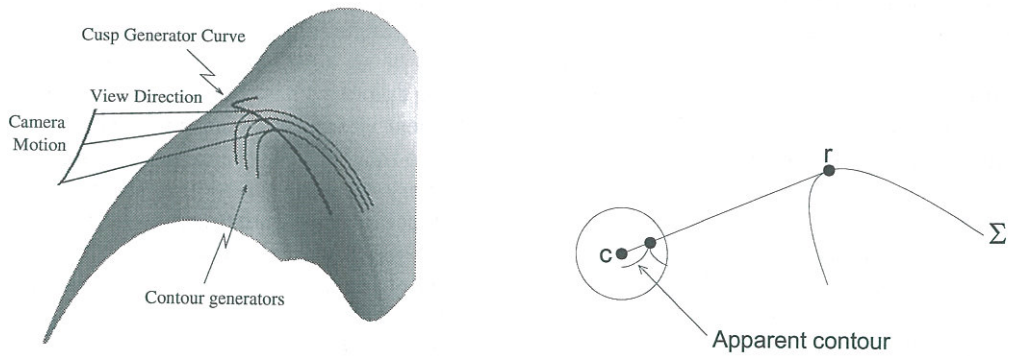

Figure 2. Left: three viewing positions $\mathbf{c}(t)$, all of which produce cusps on the apparent contours because some viewline (ray) from $\mathbf{c}(t)$ is tangent to the corresponding contour generator Σ. The cusp generator curve is labelled L. Right: A single contour generator Σ as in the figure above produces a cusp on the apparent contour when the viewline is tangent to Σ.

Although the cusp points are difficult to detect by photometric methods in video images of opaque objects they are visible in the images of transparent objects and in X-ray imaging. This is not to say that they are easy to locate accurately: cusps tend to occur as a dark blur even in an X-ray image. (There is such an image in (Koenderink, 1990, p. 425).) But at least in principle, cusp points offer the possibility of being detected and tracked under viewer motion. Giblin and Soares (1988) presented a first attempt to relate local surface geometry (Gaussian and mean curvatures and principal directions) to the image motion of cusps under orthographic projection and planar viewer motion. We extend this here to arbitrary nonplanar, curvilinear viewer motion under perspective projection. We show how the image motion of the cusp can be used to induce an alternative parametrization of the surface in the vicinity of the cusp generator which can be used to recover surface depths and orientation. Remarkably this leads to simplified formulae for surface curvature which require only first-order temporal derivatives. Furthermore our simulations suggest that the formulae are fairly robust. The computation of surface curvature at non-singular apparent contour points requires second order spatial and temporal derivatives.

We also investigate the problems and ambiguities in attempting to recover egomotion from the image motion of cusp points and present the results of some simulated experiments. We indicate how global information can be obtained with certain special classes of surface and give one example; a more detailed treatment of this topic will appear elsewhere (Fletcher and Giblin, 1996). Some of the results in the present paper were announced in (Cipolla et al., 1995).

2. Viewing Geometry and Parametrization of the Surface

2.1. *Spherical Perspective Projection*

Consider the perspective projection of a point on a smooth surface M with position vector $\mathbf{r}$. The direction of a ray to the point on a smooth surface can be represented as a unit vector $\mathbf{p}$ defined by

$$\mathbf{r} = \mathbf{c} + \lambda \mathbf{p} \tag{1}$$

where λ is the distance along the ray to the viewed point and $\mathbf{c}$ is the position of the projection centre of the viewer. This is equivalent to considering the imaging device as a spherical pinhole camera of unit radius. See Fig. 1.

For each viewpoint $\mathbf{c}$, the apparent contour determines a family of rays $\mathbf{p}$ emanating from the projection centre which are tangent to the surface so that

$$\mathbf{p}.\mathbf{n} = 0 \tag{2}$$

where $\mathbf{n}$ is the surface normal.

2.2. *Parametrization Using Contour Generators*

Movement of the viewpoint (projection centre) will produce different contour generators on the surface M. A moving monocular observer with position at time t given by $\mathbf{c}(t)$, will generate a one parameter family of contour generators, indexed by time. It is natural to attempt a parametrization of M which is 'compatible' with the motion of the camera centre, in the sense that contour generators M are parameter curves. That is, 't is to be one of the parameters on M', and so we want there to exist a regular (local) parametrization of M of the form $(u, t) \to \mathbf{r}(u, t)$, the set of points $\mathbf{r}(u, t_0)$, for fixed t_0, being the contour generator from viewpoint $\mathbf{c}(t_0)$. The set of points $\mathbf{p}(u, t_0)$ is the corresponding apparent contour in the unit sphere at the origin; the actual apparent contour points in space are $\mathbf{c}(t_0) + \mathbf{p}(u, t_0)$.

Note that (1) and (2) become

$$\mathbf{r}(u, t) = \mathbf{c}(t) + \lambda(u, t)\mathbf{p}(u, t),$$
$$\mathbf{p}(u, t).\mathbf{n}(u, t) = 0. \tag{3}$$

The conditions for such a parametrization to be possible are that

- $\mathbf{r}$ is not a *frontier point*, i.e., an *epipolar tangency point*. At a frontier point the epipolar plane (spanned by the velocity vector $\mathbf{c}_t(t)$ of the camera centre and the viewline $\mathbf{r} - \mathbf{c}$) coincides with the tangent plane to M. This causes the contour generators to form an envelope on M; see (Giblin and Weiss, 1995). We shall assume $\mathbf{c}_t(t).\mathbf{n} \neq 0$, which implies $\mathbf{c}_t(t)$ is not in the tangent plane to M: this rules out frontier points.
- The contour generators are nonsingular curves.

In this paper we are chiefly concerned with singular apparent contours, so we are avoiding only the situations of a 'cusp on the frontier' and of 'lips/beaks' singularities (Koenderink, 1990, p. 458). In the latter case, we can expect cusps to appear or disappear.

A special case of this was investigated in (Giblin and Soares, 1988, pp. 232–233).

Note that in the special case of the epipolar parametrization (Cipolla and Blake, 1992), we have $\mathbf{r}_t$ parallel to $\mathbf{p}$, and hence by differentiating (3) we have $\mathbf{p}_t$, $\mathbf{c}_t$ and $\mathbf{p}$ coplanar, i.e., $[\mathbf{p}_t, \mathbf{c}_t, \mathbf{p}] = 0$. We shall see later than when following cusps this triple scalar product is *never* zero.

2.3. *Viewer and Reference Coordinate Systems*

Note that $\mathbf{p}$ is the direction of the ray in the fixed reference/world frame for 3-space. It is determined by a spherical image position vector $\mathbf{q}$ (the direction of the ray in the camera/viewer co-ordinate system) and the orientation of the camera co-ordinate system relative to the reference frame. For a moving observer the viewer co-ordinate system is continuously moving with respect to the reference frame. The relationship between $\mathbf{p}$ and $\mathbf{q}$ can be conveniently expressed in terms of a rotation operator $R(t)$ ((Cipolla and Blake, 1992, Section 2.4) where our $\mathbf{p}$ appears as $\mathbf{Q}$ and our $\mathbf{q}$ as $\tilde{\mathbf{Q}}$):

$$\mathbf{p} = R(t)\mathbf{q}. \tag{4}$$

If the frames are defined so that instantaneously, at time $t = 0$, they coincide, i.e.,

$$\mathbf{p}(0) = \mathbf{q}(0) \tag{5}$$

and have a relative rotational velocity of $\Omega(t)$, then

$$\Omega \wedge \mathbf{q} = R_t\mathbf{q} \tag{6}$$

The relationship between temporal derivatives of measurements made in the camera co-ordinate system and those made in the reference frame is then given instantaneously at time $t = 0$ by (differentiating (4)):

$$\mathbf{p}_t = \mathbf{q}_t + \Omega \wedge \mathbf{q} \tag{7}$$

where the subscripts denote differentiation with respect to time and $\wedge$ denotes a vector product.

3. Static Properties of the Apparent Contour and Its Cusp

3.1. *Tangents and Normals*

It is well known (Cipolla and Blake, 1992) that the surface normal is recoverable from one non-singular apparent contour. We recall here the reasons for this and go on to consider the case where the apparent contour is singular.

From (3) we have

$$\mathbf{r}_u = \lambda_u\mathbf{p} + \lambda\mathbf{p}_u. \tag{8}$$

Thus $\mathbf{p} \wedge \mathbf{r}_u$ is parallel to $\mathbf{p} \wedge \mathbf{p}_u$. We have the following easy consequences of this:

- $\mathbf{p} \wedge \mathbf{r}_u$ is parallel to the normal to M so long as $\mathbf{p}$ is not parallel to $\mathbf{r}_u$.
- $\mathbf{p} \parallel \mathbf{r}_u$ if and only if the viewline is along the tangent to the contour generator, which happens if and only if the apparent contour is singular, i.e., if and only if $\mathbf{p}_u = 0$ (since $u \to \mathbf{p}(u, t)$ parametrizes the apparent contour, and $\mathbf{p}_u$ is along the tangent to the apparent contour at a nonsingular point). This also occurs if and only if the viewline is along an *asymptotic direction* (Koenderink, 1990, p. 439).
- $\mathbf{p} \wedge \mathbf{p}_u$ is parallel to the normal to the apparent contour provided $\mathbf{p}_u \neq 0$. Hence:
- *The normals to M and to the apparent contour are parallel in the general situation of a nonsingular apparent contour.*

At singular points we must look for a formula for the (limiting) tangent direction other than $\mathbf{p}_u$, and consequently a different formula for the normal from $\mathbf{p} \wedge \mathbf{p}_u$.

Proposition. *Assume as above that $\mathbf{p}_u = 0$. Provided $\mathbf{p}_{uu} \neq 0$, which will always be so at an ordinary cusp point, $\mathbf{p}_{uu}$ is in the direction of the cuspidal tangent. (In fact it points 'into' the cusp.) See Fig. 3.*

In particular $\mathbf{p}_{uu}$ is perpendicular to $\mathbf{p}$ when $\mathbf{p}_u = 0$ and the normal to the apparent contour (perpendicular to the cuspidal tangent) is in the direction $\mathbf{p} \wedge \mathbf{p}_{uu}$.

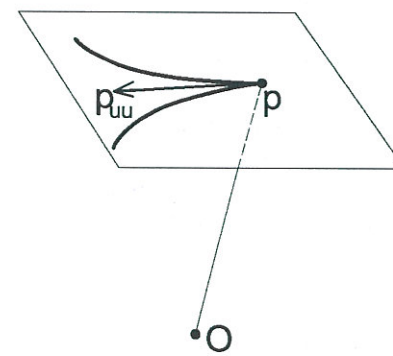

Figure 3. A cusp on the apparent contour, where $\mathbf{p}_u = 0$ and $\mathbf{p}_{uu}$ is along the cuspidal tangent.

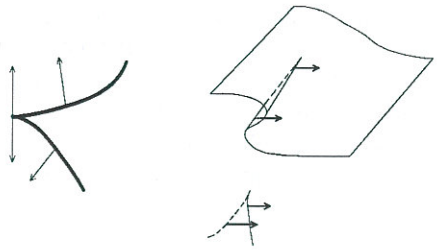

(a) (b)

Figure 4. (a) Orientation of a cusp and its normals, (b) an opaque surface where half the cusp is occluded.

Proof: See Appendix 8. □

Thus we have

$$\mathbf{p}.\mathbf{n} = 0,\ \mathbf{p}_u = 0,\ \mathbf{p}_{uu}.\mathbf{p} = 0,\ \mathbf{p}_{uu}.\mathbf{n} = 0, \quad (9)$$

where the first equation always holds and the rest apply to points where the apparent contour is singular.

Suppose that the cusp is oriented, as in Fig. 4(a). At nonsingular points we can follow the usual convention of turning to the left from the oriented tangent to obtain the oriented normal. However the two limiting normals *at* the cusp are then *opposite* in direction. On the other hand, when a surface projects to a cusp, as is sketched in Fig. 4(b), the 'outward' normals to the surface project in the image to normals which have the *same* limit as the cusp point is approached. If the surface M is *opaque* then one side of the cusp is hidden (dashed in Fig. 4(b)). If we know which way the surface is folded above the cusp then we can identify which way the projection of this outward normal to M points.

Later (see Section 4.2, Note 3) we shall give a way of determining, from the image, the projection of a particular normal. For the moment we note only the following.

Note on the Orientation of $\mathbf{r}_u$**.** Orient the visible branch of the cusped apparent contour as shown in Fig. 4(b) (into the cusp point $\mathbf{p}_0$), which corresponds to the point $\mathbf{r}_0$ on the surface, say. On the surface the contour generator can be oriented so as to correspond with the chosen orientation of the apparent contour. The oriented tangent at $\mathbf{r}_0$ to this contour generator then points in the *same* direction as $\mathbf{p}$, that is, $\mathbf{r}_u$ is a *positive* multiple of $\mathbf{p}$, which from (8) is the same as saying that $\lambda_u > 0$.

3.2. *A Static Formula for the Gauss Curvature*

There is a well-known 'static' formula for the Gauss curvature K of a surface in terms of the (geodesic) curvature κ^p of the apparent contour on the image sphere and the 'transverse' curvature κ^t of the surface, that is, the normal curvature of M in the direction of the visual ray. The formula, due to Koenderink (see (Cipolla and Blake, 1992, p. 92)) is

$$K = \kappa^p \kappa^t / \lambda.$$

In the situation of a singular apparent contour the numerator takes the form $K = \infty \times 0$ since an ordinary cusp has *infinite* curvature and the normal curvature of a surface in an asymptotic direction is always zero. It is still possible to make a sensible analogue of this when the apparent contour is singular (this was done in a special case in (Giblin and Soares, 1988), Prop. 8). In fact writing ρ for $1/\kappa^p$ it can be shown that for an ordinary cusp the limit of ρ is 0 while that of $d/ds(\rho^2)$ is finite, and nonzero. Here, s is arclength along the cusped curve. Thus the appropriate thing to do is to write $K^2 = (\kappa^t)^2/(\lambda^2\rho^2)$ and then to use l'Hôpital's rule to deduce that K is the negative square root of the limit of

$$\frac{\frac{d}{ds}(\kappa^t)}{\lambda^2 \frac{d}{ds}(\rho^2)}.$$

4. Dynamic Analysis

In this section we show that by following the *cusp trajectory* in the image, we can reconstruct a surface strip together with the second fundamental form of the surface along that strip. The cusp trajectory is defined by $\mathbf{p}_u = 0$, where, as before, $\mathbf{p}$ is a function of two variables t and u. The corresponding set of points in M is called the *cusp generator curve*.

4.1. *General Properties of the Cusp Trajectory*

It should be noted straight away that the epipolar parametrization of M, where $\mathbf{r}_t$ is parallel to $\mathbf{p}$ (compare (Cipolla and Blake, 1992, p. 90)) cannot be used in a neighbourhood of cusp points. This is because the contour generator t = constant on M, and hence the vector $\mathbf{r}_u$, is actually *parallel* to $\mathbf{p}$ at a point giving a cusp on the apparent contour. We cannot have $\mathbf{r}_t$ and $\mathbf{r}_u$ parallel for a regular parametrization of M. In particular, the formula (31) in (Cipolla and Blake, 1992) for the normal curvature κ^t fails at cusp points, where $\kappa^t = 0$.

Proposition. *Assume that* $\mathbf{p}_t \neq 0$ *and that all cusps are ordinary, so that* $\mathbf{p}_{uu}$ *is certainly not zero (compare*

the Proposition in Section 3.1). *Assume further that* $\mathbf{p}_{uu}$ *is not parallel to* $\mathbf{p}_t$. *(All these conditions will hold generically.) Then*

(i) *the cusp trajectory in the image and the cusp generator curve on* M *are smooth and parametrized by* t,
(ii) *the cusp generator curve on* M *is transverse (non-tangent) to the contour generators,*
(iii) *The velocity vector of the cusp in the image sphere is equal to the vector* $\mathbf{p}_t$.
(iv) *The normal component of acceleration along the cusp trajectory in the image is given by* $\mathbf{p}_{tt}.\mathbf{n}$.

Proof: See Appendix 9. Note that if $\mathbf{p}_{uu}$ is parallel to $\mathbf{p}_t$ then either the surface point $\mathbf{r}$ is a frontier point (epipolar tangency point) or the apparent contour is undergoing a 'swallowtail transition' (Koenderink, 1990, p. 458). The latter implies that, on the surface, the cusp generator curve is *tangent* to the contour generator. More details of this kind of situation can be found in (Giblin and Weiss, 1995). □

We can make immediate use of the above Proposition to customize slightly the parametrization of M. In fact, we can choose the smooth cusp generator curve on M as the curve $u = 0$ in our parametrization of M; see Fig. 2, where this curve is marked L. This has the advantage that we have $\mathbf{p}_u(0, t) = 0$ for all values of t, so that differentiating with respect to t (for which we can put $u = 0$ first) we obtain

$$\mathbf{p}_{ut} = 0 \tag{10}$$

along the cusp trajectory in the image.

4.2. *Surface Geometry by Following Cusps*

Using (3) we obtain by differentiation and use of (9), (10) the following formulae which hold at cusp points:

$$\begin{aligned}
\mathbf{r} &= \mathbf{c} + \lambda\mathbf{p},\\
\mathbf{r}_u &= \lambda_u\mathbf{p}\\
\mathbf{r}_t &= \mathbf{c}_t + \lambda_t\mathbf{p} + \lambda\mathbf{p}_t,\\
\mathbf{r}_{uu} &= \lambda_{uu}\mathbf{p} + \lambda\mathbf{p}_{uu},\\
\mathbf{r}_{ut} &= \lambda_{tu}\mathbf{p} + \lambda_u\mathbf{p}_t,\\
\mathbf{r}_{tt} &= \mathbf{c}_{tt} + 2\lambda_t\mathbf{p}_t + \lambda_{tt}\mathbf{p} + \lambda\mathbf{p}_{tt}.
\end{aligned} \tag{11}$$

Using these formulae, and standard methods given for example in (O'Neill, 1966, pp. 210–213), we can find expressions for the Gauss curvature and mean curvature of M at points of the cusp generator curve. We state these formulae here, and make comments on them below. The proofs are in Appendix 10.

Clearly these formulae can be transformed into rotated viewer coordinates using the formulae in Section 2.3.

Proposition.

$$K = \frac{-(\mathbf{p}_t.\mathbf{n})^4}{[\mathbf{p}, \mathbf{c}_t, \mathbf{p}_t]^2},$$

$$H = \frac{\mathbf{p}_t.\mathbf{n}(\mathbf{c}_{tt}.\mathbf{n}\,\mathbf{p}_t.\mathbf{n} - \mathbf{c}_t.\mathbf{n}\,\mathbf{p}_{tt}.\mathbf{n} - 2\mathbf{p}.\mathbf{c}_t(\mathbf{p}_t.\mathbf{n})^2)}{2[\mathbf{p}, \mathbf{c}_t, \mathbf{p}_t]^2}.$$

Notes on the Formulae.

1. Recall that the standard formula for K (see (Cipolla and Blake, 1992, Section 4.3)) depends on second temporal derivatives of camera position and image, and also on the curvature of the image. It is therefore a striking feature of the above formula for K that it lacks *second* derivatives. Using the special geometry of cusp points, we have obtained a formula for Gauss curvature which depends on the first derivatives of the motion only.
2. Note that the denominator of the expressions for K and H cannot be zero (provided our assumptions, as in Section 2.2, hold); this is the opposite situation to that of the epipolar parametrization, where it is always zero.
3. The normal $\mathbf{n}$ in the above formulae is assumed to be in the direction of $\mathbf{r}_u \wedge \mathbf{r}_t$. It is not immediately clear that this direction can be found from the image. However, we show in Appendix 11 that we find the direction, at any rate for an opaque surface, as follows.

   Orient the visible part of the apparent contour towards the cusp point, taking $\mathbf{r}_u$ therefore to be a *positive* multiple of $\mathbf{p}$; compare the note on orientation in Section 3.1. Choose a normal $\mathbf{n}$ at the cusp point and consider the sign of $[\mathbf{p}, \mathbf{c}_t, \mathbf{p}_t]/\mathbf{p}_t.\mathbf{n}$. The chosen normal is along $\mathbf{r}_u \wedge \mathbf{r}_t$ (i.e., a *positive* multiple of this) if and only if this sign is positive. Thus the sign of H is unambiguous in the above formula.
4. Once we have the Gauss and mean curvatures at a point where the apparent contour gives a cusp we have essentially determined the second fundamental form of the surface at that point (see below). Thus by following cusps we can recover a surface strip

along the cusp generator curve, together with the second fundamental form of the surface along that strip.

Think of a surface in 'Monge form', $z = f(x, y)$ with f, f_x, f_y all vanishing at $x = y = 0$, so that the tangent plane to the surface at the origin is the plane $z = 0$. Let one asymptotic direction be along the x-axis. Then the surface has the form

$$z = \frac{1}{2}(2f_{xy}xy + f_{yy}y^2) + \text{higher order terms},$$

the derivatives being evaluated at $x = y = 0$. Knowing $K = -f_{xy}^2$ and $H = f_{yy}/2$ we know the second order terms, and hence the second fundamental form, apart from an ambiguity of sign in f_{xy}.

In fact, in our situation of working at the cusp points, we can eliminate this ambiguity. This is sketched in Appendix 12.

5. Note the interpretations of $\mathbf{p}_t.\mathbf{n}$ and $\mathbf{p}_{tt}.\mathbf{n}$ as the normal components of velocity and acceleration along the cusp trajectory, as in the Proposition in Section 4.1, (iii) and (iv) above. An equivalent expression for the denominator of K is given in Lemma 2 in Appendix 10. Since $\mathbf{p} \wedge \mathbf{p}_t$ is along the *normal*, $\mathbf{n}_c$ say, to the cusp trajectory, we could also write this denominator as $(\mathbf{n}_c.\mathbf{c}_t \|\mathbf{p}_t\|)^2$.
6. A special case of the formulae above for K and H was obtained in (Giblin and Soares, 1988). It can be shown fairly readily that these special results follow from ours.
7. In fact the formulae of the above Proposition do not depend on *following* cusps, merely on *starting* at a cusp point. The instantaneous veclocities can be measured for any surface curve parametrized by time t and starting at this point and the formulae then hold *at this point.*

4.3. *Image Velocity of a Cusp Point*

Finally in this section we consider the image velocity of the cusp. Recall from Section 4.1, (iii) of the Proposition, that we can measure $\mathbf{p}_t$ by measuring the velocity of the cusp along its trajectory in the image. Now write $\mathbf{t}$ for the tangent to the cusp, which we can define as $\mathbf{n} \wedge \mathbf{p}$. We have

$$\begin{aligned}(\mathbf{p}_t.\mathbf{n})(\mathbf{c}_t.\mathbf{t}) - (\mathbf{c}_t.\mathbf{n})(\mathbf{p}_t.\mathbf{t}) &= (\mathbf{t} \wedge \mathbf{n}) \wedge \mathbf{c}_t).\mathbf{p}_t \\ &= [\mathbf{p}, \mathbf{c}_t, \mathbf{p}_t].\end{aligned}$$

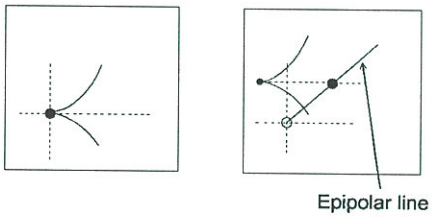

Figure 5. Moving cusp versus surface marking (large dot): the marking moves along the epipolar line while the cusp has relative motion along the tangent of magnitude $\mathbf{c}_t.\mathbf{n}/(\lambda^2\sqrt{(-K)})$.

Recall the standard depth formula (Cipolla and Blake, 1992)

$$\lambda = -\frac{\mathbf{c}_t.\mathbf{n}}{\mathbf{p}_t.\mathbf{n}}. \tag{12}$$

Rearranging and using (12) and the Proposition in Section 4.2 we find:

Proposition. *The components of image velocity of the cusp are given by*

$$\begin{aligned}\mathbf{p}_t.\mathbf{n} &= -\frac{\mathbf{c}_t.\mathbf{n}}{\lambda}, \\ \mathbf{p}_t.\mathbf{t} &= -\frac{\mathbf{c}_t.\mathbf{t}}{\lambda} \pm \frac{\mathbf{c}_t.\mathbf{n}}{\lambda^2\sqrt{-K}},\end{aligned}$$

where the sign, $\pm$, *is that of* $[\mathbf{p}, \mathbf{c}_t, \mathbf{p}_t]$.

Note that the formula for $\mathbf{p}_t.\mathbf{n}$ is *the same* as we would get by following the end-point of a surface marking, rigidly attached to the surface, while the *first* term of $\mathbf{p}_t.\mathbf{t}$ is the one we should expect from a surface marking. The second term represents the contribution of the surface, when we are following a cusp, which is not rigidly attached to the surface. If K is large, then this term is insignificant; the limiting case of '$K = \infty$' corresponds to that of a space curve or surface marking. See Fig. 5 which illustrates schematically the cusp moving away from the epipolar line in the image sphere, here drawn as a plane.

5. Motion Constraints

In this section we address the question: given only the locus of apparent contour cusps in the image sphere (using say the rotated $\mathbf{q}$ coordinates), can we place any constraints on the viewer motion? In fact we show that, using the locus of cusps as a parametrized curve $\mathbf{q}(t)$

in the sphere, and using also the normal lines to the cusps, there cannot be any constraint on the motion. Explicitly, we claim the following, where t is a real number lying in some (small) open interval $t_1 < t < t_2$.

Theorem. *Suppose that* $\mathbf{q}(t)$, $\mathbf{n}(t)$ *are given smooth families of orthogonal unit vectors, that* $R(t)$ *is a smooth family of* 3*-dimensional rotations, and that* $\mathbf{c}(t)$ *is a smooth space curve. Then we can find a smooth surface* M *in* 3*-space for which* $\mathbf{q}(t)$ *is the locus of cusps of apparent contours arising from camera centres* $\mathbf{c}(t)$*, with rotated coordinates* $\mathbf{q}(\mathbf{p} = R(\mathbf{q})$ *in the usual notation) and* $R(t)(\mathbf{n}(t))$ *is the normal to the apparent contour at the cusp point.*

Proof: Let $\mathbf{p}(t) = R(t)\mathbf{q}(t)$ and replace also $\mathbf{n}$ by its rotated form $R(t)\mathbf{n}(t)$ (we shall continue to use $\mathbf{n}$). We then seek a surface M with the following properties:

- for each t, there is a point $\mathbf{r}(t) = \mathbf{c}(t) + \lambda(t)\mathbf{p}(t)$ on M for some $\lambda(t)$,
- the normal to M at $\mathbf{r}(t)$ is $\mathbf{n}(t)$,
- for each t, the vector $\mathbf{p}(t)$ is in an asymptotic direction at $\mathbf{r}(t)$ (this ensures that the apparent contour at 'time' t has a cusp at the apparent contour point $\mathbf{c}(t) + \mathbf{p}(t)$).

There is no choice for the function λ, since we require (using subscripts to denote differentiation as usual) $\mathbf{r}_t = \mathbf{c}_t + \lambda\mathbf{p}_t + \lambda_t\mathbf{p}$, and since $\mathbf{n}(t)$ is required to be normal to the surface, we deduce the usual formula

$$\lambda(t) = -\mathbf{c}_t.\mathbf{n}/\mathbf{p}_t.\mathbf{n}, \tag{13}$$

noting here that $\mathbf{p}$ is a function of *one* variable t, since it gives the position of the cusp (in unrotated $\mathbf{p}$ coordinates).

We now have a space curve $\mathbf{r}(t)$, and, along that curve, we shall require our surface M to have normal $\mathbf{n}(t)$ (for this is parallel to the apparent contour normal in the unrotated coordinates). This gives us a 'surface strip' in the language of Koenderink (1990).

The final requirement on M is that, at each point $\mathbf{r}(t)$, an asymptotic direction is in the specified direction $\mathbf{p}(t)$. This amounts to saying that, in the direction $\mathbf{p}(t)$, the sectional curvature of M is zero, that is the section of M by the plane through $\mathbf{r}(t)$ containing $\mathbf{p}(t)$ and $\mathbf{n}(t)$ has an (ordinary) inflexion at $\mathbf{r}(t)$. There is no difficulty in constructing an M with this property, so long as the asymptotic direction does not actually coincide with the tangent to the curve $\mathbf{r}(t)$. But in that case it is easy to check that the locus of cusps $\mathbf{p}(t)$ in the image sphere would be singular. (Another way of thinking of this reconstruction is to say that we are specifying the second fundamental form of M at each point of a curve on M, for specifying one asymptotic direction and the derivative of the normal in a *different* direction (along the curve) is precisely enough to fix the second fundamental form. Of course there is no claim here that the surface constructed is unique, away from the curve $\mathbf{r}(t)$.) □

6. Experiments

We have performed many simulations using the method of following cusps, and we briefly describe here some of them. In the first, we seek only to recover the Gauss curvature from a cusp locus in the image sphere, while in the others we assume that the object surface is of a special kind and use cusp tracking to do a global reconstruction of the surface. We have reported on these global experiments in detail elsewhere (Fletcher and Giblin, 1996). We regard the present series of experiments as a first attempt to test the viability of the above theory; in particular we do not claim to have overcome the technical problems of locating cusps, or contour-endings, in images.

The method adopted for the experiments is as follows. Rather than taking an explicit surface and camera motion, and calculating the cusp generator curve and cusp locus, we used the result of Section 5 which says that we can take a cusp locus $\mathbf{p}(t)$, normal vectors $\mathbf{n}(t)$ and camera motion $\mathbf{c}(t)$ and be sure that there is a surface 'out there' which fits this data. For simplicity $\mathbf{c}(t)$ was taken as a straight line. The cusp locus was always taken as an explicit curve in the image sphere, given in terms of 'latitude' θ and 'longitude' ϕ:

$$\mathbf{p}(t) = (\cos\theta\cos\phi, \cos\theta\sin\phi, \sin\theta).$$

Here θ, ϕ are functions of t which can conveniently be taken to be simple polynomials. We also took a family of normal vectors $\mathbf{n}(t)$ (subject only to the condition that $\mathbf{n}(t)$ had to be perpendicular to $\mathbf{p}(t)$).

To simulate the uncertainty in the position of the cusp, we added noise to the cusp positions $\mathbf{p}(t)$. Thus we thought of each cusp as a blurry circular blob surrounding its actual position, and we took a random position inside this blob as the measured position of the cusp. It seems to us probable that the blob would be, in real life, more elliptically shaped, with the long axis

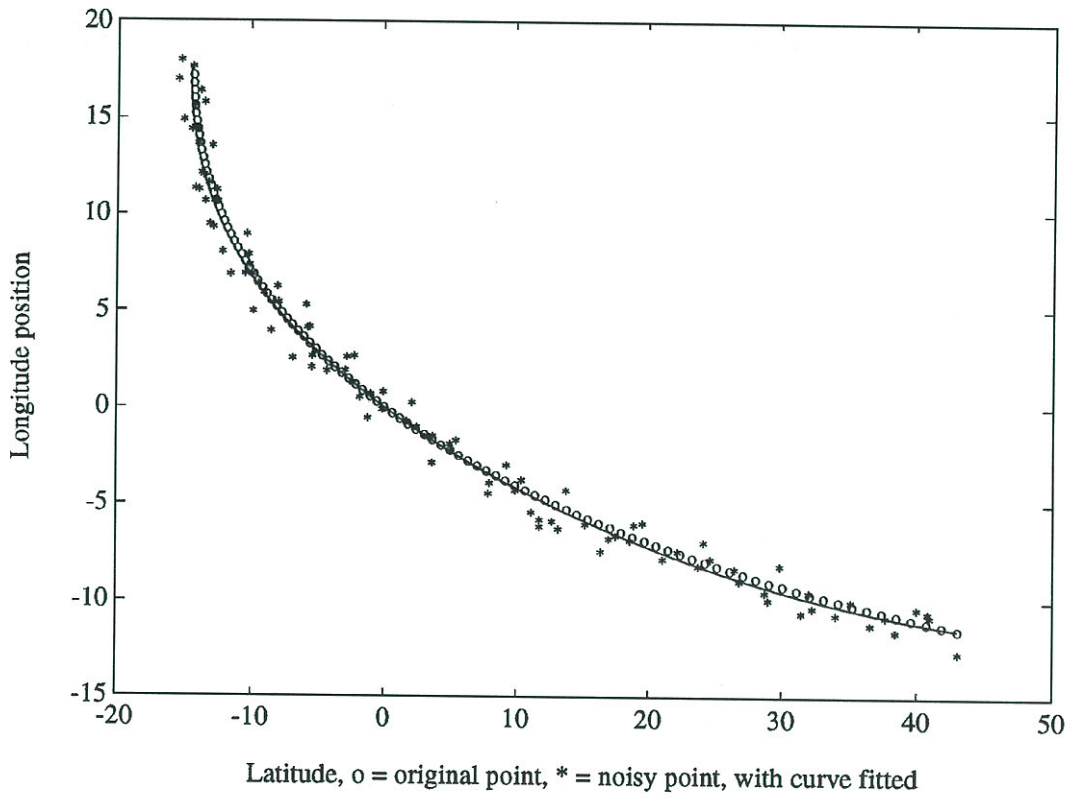

Figure 6. A cusp locus on the image sphere, given by latitude and longitude. Noise has been added to the data and the noisy data fitted by a polynomial curve. Because of the method of simulation we have not shown the cusped profiles themselves.

along the tangent to the cusp: there should be greater uncertainty in this direction than in the normal direction. We took some account of this in decreeing that the uncertainty in the normal $\mathbf{n}(t)$ should be *smaller* than that in the position $\mathbf{p}(t)$.

Thus we produced a scattering of a large number of points which represented the measured positions of the cusp: see Fig. 6, which is a picture of the θ, ϕ plane parametrizing the sphere. In order to use the formulae of Section 4.2 we had to fit a curve to all this noisy data so that derivatives could be calculated. In practice it would be necessary to try various degrees of polynomial to fit the data; because the cusp loci produced in our experiments were not very wavy, we found that a least-squares fit parametrized curve in which each coordinate θ, ϕ was of degree 4 in the parameter worked very well, and in fact degree 3 was nearly as good. The result of fitting a curve is also shown in Fig. 6; as can be seen, the fitted curve is a reasonable approximation to the original cusp positions, though the fit naturally becomes steadily worse as the noise is increased. The fitted curve was used to calculate the derivatives used in the formulae of Section 4.2. Even when the fitted curve is a good approximation to the cusp locus, we can expect the derivative of the fitted curve to be a worse approximation to the true derivative. Luckily, using our formulae, only *first* derivatives are needed. This seems to contribute to the relative robustness of the method.

A similar curve-fitting exercise turned the noisy normal vectors into a curve in the θ, ϕ plane. For these experiments we took it that $\mathbf{c}(t)$ was known exactly.

6.1. *Recovery of Gauss Curvature*

In these experiments, we calculated the exact Gauss curvature of the simulated surface along the cusp generator curve using the formula of Section 4.2. Note that, since we took a closed form for $\mathbf{p}(t)$, we could calculate the derivatives $\mathbf{p}_t$ explicitly in this exact calculation.

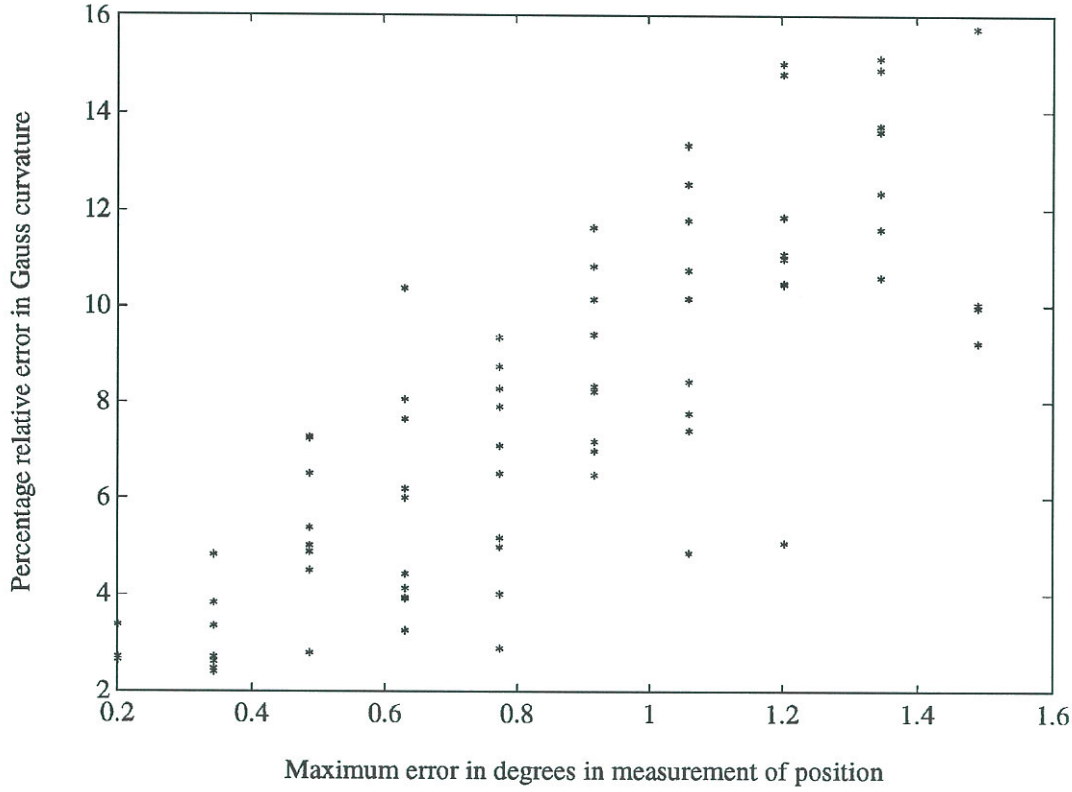

Figure 7. The results of several simulations, each with increasing amounts of noise, showing the resulting relative percentage error in measuring Gauss curvature.

As above, curves were fitted to the noisy cusp and normal data and these curves used to calculate the approximate Gauss curvature of the surface. In this, it is an advantage that only *first* derivatives are needed, in contrast with the formulae of (Cipolla and Blake, 1992). In Fig. 6 we show a typical cusp locus in the ϕ, θ coordinate plane (angles being in degrees!), and the noisy data together with a curve fitted to this data. In Fig. 7 we show the results of about 10 experiments with different cusp and normal loci, for each of which we took an increasing amount of added noise. That is, the measured cusp positions were assumed to lie at random positions in steadily larger circles centred at the actual cusp points. Ignoring the ends of the cusp locus, if we take a typical width to be about 40°, then a noise level of 1° in each of the angular coordinates represents a maximum error of about 1.5° or nearly 4%. Thus each true cusp point is surrounded by a blurry region of angular width about 4% of the total angular spread of the cusp locus in the image sphere. The 'estimated position' of the cusp is a random point within this blurry region. This seems typically to produce about a 10% error in the Gauss curvature, still giving useful surface information. Further the error does not appear to increase more than linearly with the maximum noise.

In terms of pixels, for a camera with a focal length of 20 mm and pixel density of 500 pixels per 5 mm, we find that an angular separation of 0.03 degrees is about 1 pixel. So it will be seen that we are taking very large noise levels in these experiments, to allow for the known difficulty in localising cusps and contour endings.

6.2. *Special Classes of Surface*

There are several special classes of surface where 'following the cusp' can given *global* information. We give a few details here of three of these special classes; detailed experiments and results are reported on elsewhere (Fletcher and Giblin, 1996). Although this is an 'experimental' section, we also need to establish a few theoretical (and not completely standard) facts about special surfaces in order to apply our methods to global reconstruction.

Ruled Surfaces. We use the formulae of Section 4.2 to find both the Gauss curvature K and the mean curvature H of the surface along the cusp generator curve. A ruled surface consists of straight lines, usually called 'generators' but here we use the word 'ruling' to avoid confusion with contour and cusp generators. Recall that, at each point, one asymptotic direction on a ruled surface is along the ruling through that point. In our case, the other asymptotic direction is along the view direction, since we are viewing cusps of apparent contours, and we can make use of a well-known formula for the angle α between the asymptotic directions on any surface: $\tan\alpha = \sqrt{-K}/H$. (See (O'Neill, 1966, p. 225).) Our angle α is 2ϑ where ϑ is the angle in (O'Neill, 1966). Also $K = k_1k_2$, $H = \frac{1}{2}(k_1 + k_2)$ where k_1, k_2 are the principal curvatures. The formula for $\tan\alpha$ follows easily from this and the formula $\tan^2\vartheta = -k_1/k_2$ in (O'Neill, 1966). The tangent plane to the surface is spanned by the vectors $\mathbf{p}$ and $\mathbf{p}\wedge\mathbf{n}$, $\mathbf{p}$ being along the viewline which is asymptotic. The other asymptotic direction, along the ruling, is therefore

$$\mathbf{p}\cos\alpha + \mathbf{p}\wedge\mathbf{n}\sin\alpha.$$

It is an easy matter therefore to construct the ruling through each surface point.

We have done this for various ruled surfaces, adding noise to the image and estimating the ruling from this noisy data. The derivatives involved were estimated by the same method as in Section 6.1. Note that we now need second temporal derivatives of $\mathbf{p}$ in order to use the formula for H in Section 4.2. Even with substantial amounts of noise (a maximum angular error of 1.5° in an angular width of around 50°) we still found that the reconstructed surface was a useful approximation to the original. We have tried to illustrate this in Fig. 8 which shows the true surface as a shaded and opaque surface and the reconstructed ruling as black lines. In Fig. 9 we show an image cusp in a projection of a ruled surface, in opaque mode (left) and transparent mode (right, where the cusp can be seen at the left of the central darker area).

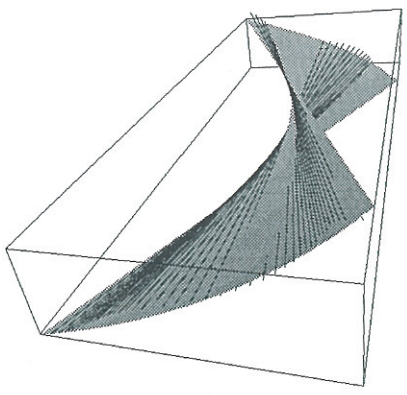

Figure 8. Ruled surface and its reconstruction from the cusp locus.

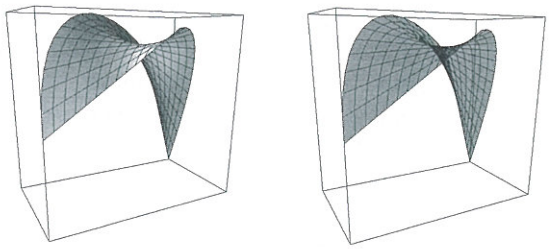

Figure 9. Projection of a ruled surface showing a cusp on the profile: on the left the surface is opaque and the cusp is an apparent contour ending, while on the right the surface is transparent and the cusp is at the left of the central darker area.

Surfaces of Revolution. Surfaces of revolution have circular 'parallel sections', namely the sections by the family of parallel planes all of which are perpendicular to the axis of revolution. It can be shown that, if there is a cusp generator point on a particular parallel section then there will be exactly one other such point on that section: the cusp generator points occur in pairs. In the image we therefore have pairs of cusps corresponding to points on the same parallel section. If there are more than two cusps in one image then we can assist the pairing by calculating the Gauss curvature, which will be the same at the pair of points on the same section. Reconstructing the cusp generator points in pairs, using the distance formula (13), we can find the surface normals at these points. These will theoretically intersect on the axis of revolution; in practice we can find their points of nearest approach and estimate the axis, and hence the radius function. It is also possible to use a method similar to that in Section 6.2 to estimate asymptotic directions as a check on the calculations.

Tubular Surfaces. A tubular surface (canal surface) is obtained from a 'core' curve C by taking a circle of fixed radius r in the normal plane to C at each point. These circles sweep out the tubular surface. If K, H are as usual the Gauss and mean curvatures of such a surface then it can be shown that

$$r = \frac{H \pm \sqrt{H^2 - K}}{K}.$$

Now K and H can be estimated by following cusps, using the formulae of Section 4.2, and hence the radius can be estimated. As a rule the ambiguous sign in r can be eliminated by using more than one circle, since r must have the same value for each. Further, we can obtain the second asymptotic direction (besides the viewline), as in Section 6.2, and hence the principal directions at the cusp generator points, since these bisect the two asymptotic directions. One of these principal directions is along the tangent to the circle of radius r, so up to a choice of principal directions we can recover the circle itself and hence the tubular surface.

7. Conclusions

In this paper we have shown how to recover a strip of surface and its second fundamental form in the vicinity of the cusp generator curve by following cusps under known viewer motion. The epipolar parameterisation which has been successfully exploited to recovery surfaces at non-singular profile points is degenerate at cusps and ill-conditioned in their immediate vicinity. Cusp points, however, have the advantage that they can be tracked under viewer motion and this was used to induce an alternative parameterisation based on the trajectory of the cusp in the image and the cusp generator curve on the surface. This yields alternative expressions for the recovery of depth, surface orientation and curvature from known viewer motion and measurements of the cusp point velocity and acceleration. Remarkably the expressions for Gaussian curvuture are extremely simplified, only depending on image velocities.

Following cusps can also be used to discriminate them from surface markings. Unlike a surface marking—whose projection is constrained by the epipolar constraint to epipolar lines/great-circles in consequent images—a cusp point has an additional component of image motion along the cuspidal tangent which depends on surface Gaussian curvature. Cusps will not generally project onto the epipolar lines/great-circles induced in new viewpoints and this can be used in their discrimination.

We have given simulated experiments showing how the measurement of Gauss curvature and the reconstruction of ruled surfaces is affected by noise in the image. Other classes of surface (tubular surfaces, surfaces of revolution) can also be reconstructed globally using cusp tracking.

Can following cusps be used to constrain the viewer motion? Unfortunately we have seen that, irrespective of the number of cusps which can be detected and tracked, their image trajectories alone can not be used to determine viewer motion. However it seems likely that constraints on viewer motion are available from the image motion of the apparent contour. *Frontier points* or epipolar tangencies—a third degenerate case of the epipolar parameterisaton—provide constraints on ego-motion even though the contour generators are not fixed in space. A very special case was covered in (Giblin et al., 1994). Efficiently detecting these in the presence of arbitrary viewer translations and rotations remains to be investigated, but preliminary results, reported in (Cipolla et al., 1995) are encouraging.

It is tempting to track T-junctions in the hope that they provide additional information in the same way that cusps do. The T-junction can be tracked and its velocity obtained *in any direction*. Unfortunately, tracking a T- junction does not appear to give us any advantage over using the two separate branches of the T.

For a single branch of apparent contour, the speed normal to the apparent contour can be measured and, in the fixed $\mathbf{p}$ coordinate system, is $\mathbf{p}_t.\mathbf{n}$. For a moving T-junction, we can measure the speed of the junction and so deduce the *tangential* speed of the apparent contour. However, when the two branches of the apparent contour are transverse (non-tangential), we have two normal velocities which can be measured, namely, those in directions normal to the two branches. Calculation shows that the formula obtained from these two measurements for the tangential velocity is identical with the formula obtained from tracking the T-junction. Thus by equating the two ways of obtaining the tangential velocity we cannot deduce any information about the motion or the surface.

Acknowledgments

The authors acknowledge the support of the Isaac Newton Institute for Mathematical Sciences, Cambridge. The computer pictures were produced using the 'Liverpool Surfaces Modelling Package' written by Dr. Richard Morris. Giblin acknowledges SERC/EPSRC Grant GR/H59855; Fletcher is supported by an EPSRC studentship.

Appendix

8. *Cuspidal Tangent*

Here, we prove the Proposition in 3.1. At nonsingular points of the apparent contour the tangent direction is

that of $\mathbf{p}_u$, or of the unit vector $\widehat{\mathbf{p}_u} = \mathbf{p}_u/\|\mathbf{p}_u\|$. Note that at an ordinary cusp the limit of this *does* exist. By l'Hôpital's rule, the limit coincides with the limit of $\mathbf{p}_{uu}/\widehat{\mathbf{p}_u}.\mathbf{p}_{uu}$, the denominator here being the derivative of $\|\mathbf{p}_u\|$. Now at an ordinary cusp, by definition, the second and third derivatives $\mathbf{p}_{uu}$, $\mathbf{p}_{uuu}$ are independent (compare (Bruce and Giblin, 1992, p. 155)), and in particular $\mathbf{p}_{uu}$ is non-zero. Thus the limit of the above expression has direction that of $\mathbf{p}_{uu}$, i.e., the limiting tangent has the latter direction.

9. *Cusp Trajectory*

Here, we prove the Proposition in 4.1.

(i) Consider the function

$$g(u, t) = [\mathbf{p}, \mathbf{p}_u, \mathbf{p}_t],$$

the quantity on the right being a scalar triple product. Then certainly the values of (u, t) giving cusps are *contained* in the set of zeroes of g. Furthermore with the hypotheses of the proposition, t can be used as a parameter on $g = 0$, for, at points where $\mathbf{p}_u = 0$, we have $g_u = [\mathbf{p}, \mathbf{p}_{uu}, \mathbf{p}_t]$. This is zero if and only if $\mathbf{p}$, $\mathbf{p}_{uu}$ and $\mathbf{p}_t$ are coplanar. But by hypothesis these vectors are all nonzero, and the second and third are both perpendicular to $\mathbf{p}$. So coplanarity is equivalent to $\mathbf{p}_{uu} \parallel \mathbf{p}_t$. Thus $g_u \neq 0$ and the implicit function theorem says that t is a parameter on $g = 0$.

We now need to project $g = 0$ to the image sphere, that is consider $\mathbf{p}(g^{-1}(0))$, and ask when t is a parameter on this set, which is the cusp trajectory in the image sphere. This trajectory will be smooth provided there is no nonzero vector lying in both the kernel of $Dg(u, t)$ and $D\mathbf{p}(u, t)$, D standing for derivative map. Taking local coordinates on the image sphere, it is not hard to check that the condition for smoothness is just the same as $g_u \neq 0$.

(ii) Letting $\delta(t) = \mathbf{r}(U(t), t)$ be the cusp generator curve on M, we have $\delta' = \mathbf{r}_u U' + \mathbf{r}_t$. The tangent to the contour generator is simply $\mathbf{r}_u$ in this notation, and $\delta' \wedge \mathbf{r}_u = \mathbf{r}_t \wedge \mathbf{r}_u \neq 0$, since u, t do form a regular system of local coordinates on M.

(iii) Note that $\mathbf{p}_u(U(t), t) = 0$ for some function U, and, differentiating with respect to t,

$$\frac{d}{dt}(\mathbf{p}(U(t), t)) = \mathbf{p}_u U' + \mathbf{p}_t = \mathbf{p}_t, \qquad (14)$$

at all points where $\mathbf{p}_u = 0$. The first term in this equation is by definition the velocity of the cusp, along the cusp trajectory, and this equals the last term $\mathbf{p}_t$.

The 'bad situation' is when this tangent is along the cuspidal tangent itself, i.e., when $\mathbf{p}_{uu}$ is parallel to $\mathbf{p}_t$ (or indeed when $\mathbf{p}_t = 0$). Then we may expect the cusp trajectory itself to have a cusp. Note that the set $g = 0$ includes, besides the cusp points of apparent contours, those points where $\mathbf{p}_u$ is parallel to $\mathbf{p}_t$. Thus our result shows that, with the hypotheses of the proposition, all these sets are smooth. The set $\mathbf{p}_u \parallel \mathbf{p}_t$ is the set of *envelope points of apparent contours in the image sphere.*

(iv) We have

$$\frac{d^2}{dt^2}\mathbf{p}(U(t), t) = \mathbf{p}_u U'' + \mathbf{p}_{uu}(U')^2 + 2\mathbf{p}_{tu}U' + \mathbf{p}_{tt}.$$

Now under our assumptions, $\mathbf{p}_u$ and $\mathbf{p}_{tu}$ are both zero, so, at points of the curve of cusps, we have

$$\frac{d^2}{dt^2}\mathbf{p}(U(t), t) = \mathbf{p}_{uu}(U')^2 + \mathbf{p}_{tt}.$$

Note that the left hand side, that is the acceleration of the cusp point, is *not* equal to $\mathbf{p}_{tt}$: there is a component in the direction of the tangent line to the cusp, which is along $\mathbf{p}_{uu}$ by the Proposition in Section 3.1. However, if we take the scalar product with the normal vector n we have (see (9)),

$$\left(\frac{d^2}{dt^2}\mathbf{p}(U(t), t)\right).\mathbf{n} = \mathbf{p}_{tt}.\mathbf{n}.$$

as required.

10. *Formulae for K and H*

Here, we prove the Proposition in Section 4.2.

The formulae in (O'Neill, 1966, pp. 210–213) for Gauss curvature K and mean curvature H are:

Lemma 1. *Let* $E = \mathbf{r}_u.\mathbf{r}_u$, $F = \mathbf{r}_u.\mathbf{r}_t$, $G = \mathbf{r}_t.\mathbf{r}_t$, $L = \mathbf{r}_{uu}.\mathbf{n}$, $M = \mathbf{r}_{ut}.\mathbf{n}$, $N = \mathbf{r}_{tt}.\mathbf{n}$. *Then*

$$K = \frac{LN - M^2}{EG - F^2}, \quad H = \frac{GL + EN - 2FM}{2(EG - F^2)}.$$

Using (9) we find

$$E = \mathbf{r}_u.\mathbf{r}_u = \lambda_u^2,$$
$$F = \mathbf{r}_u.\mathbf{r}_t = \lambda_u(\mathbf{p}.\mathbf{c}_t + \lambda_t),$$
$$G = \mathbf{r}_t.\mathbf{r}_t = (\mathbf{c}_t + \lambda_t\mathbf{p} + \lambda\mathbf{p}_t)^2. \qquad (15)$$

Hence the expression occurring in the denominators of K, H is

$$EG - F^2 = \lambda_u^2((\mathbf{c}_t + \lambda\mathbf{p}_t)^2 - (\mathbf{p}.\mathbf{c}_t)^2). \qquad (16)$$

Also

$$L = \mathbf{r}_{uu}.\mathbf{n} = \lambda\mathbf{p}_{uu}.\mathbf{n} = 0,$$
$$M = \mathbf{r}_{ut}.\mathbf{n} = \lambda_u\mathbf{p}_t.\mathbf{n},$$
$$N = \mathbf{r}_{tt}.\mathbf{n} = (\mathbf{c}_{tt} + 2\lambda_t\mathbf{p}_t + \lambda\mathbf{p}_{tt}).\mathbf{n} \qquad (17)$$

It is noteworthy that when using the formulae of Lemma 1 for K and H, the occurrences of λ_t and λ_u all disappear. After using (12) to substitute for λ in (16), we want to simplify the expression

$$((\mathbf{p}_t.\mathbf{n})\mathbf{c}_t - (\mathbf{c}_t.\mathbf{n})\mathbf{p}_t)^2 - (\mathbf{p}.\mathbf{c}_t\ \mathbf{p}_t.\mathbf{n})^2. \qquad (18)$$

Lemma 2. *The above expression* (18) *is equal to each of*

$$[\mathbf{p}, \mathbf{c}_t, \mathbf{p}_t]^2 \quad \text{and} \quad \|\mathbf{c}_t \wedge \mathbf{p}_t\|^2.$$

Note. This makes it obvious that the expression (16) is *positive.*

Proof: First it is easy to check directly that the expression (18) is unchanged if we add any multiple of $\mathbf{p}$ to the vector $\mathbf{c}_t$. From this it follows that we can replace $\mathbf{c}_t$ by its projection, $\mathbf{v}$ say, to the plane perpendicular to $\mathbf{p}$. In that case the second squared term in (18) vanishes and we are left with $((\mathbf{p}_t.\mathbf{n})\mathbf{v} - (\mathbf{v}.\mathbf{n})\mathbf{p}_t)^2$, which equals $(\mathbf{n} \wedge (\mathbf{v} \wedge \mathbf{p}_t))^2$. Now $\mathbf{v}$ and $\mathbf{p}_t$ are both perpendicular to $\mathbf{p}$, so $\mathbf{v} \wedge \mathbf{p}_t$ is parallel to $\mathbf{p}$ and so perpendicular to $\mathbf{n}$. Hence

$$(\mathbf{n} \wedge (\mathbf{v} \wedge \mathbf{p}_t))^2 = \|\mathbf{v} \wedge \mathbf{p}_t\|^2 = ((\mathbf{v} \wedge \mathbf{p}_t).\mathbf{p})^2,$$

the last equality holding, again, because $\mathbf{v} \wedge \mathbf{p}_t$ is parallel to $\mathbf{p}$. We have reduced (18) to the forms in the statement of the Lemma but with $\mathbf{c}_t$ replaced by $\mathbf{v}$. However adding a multiple of $\mathbf{p}$ to $\mathbf{c}_t$ does not affect these forms, so the Lemma is proved. □

Now we can write down the formulae for K, H which result from Lemmas 1 and 2. Of course, we continue to assume that we are not working at a frontier point, (see Section 2.2), so that $\mathbf{p}_t.\mathbf{n}$ and $\mathbf{c}_t.\mathbf{n}$ are nonzero.

11. *Orientation of Normals*

Here, we prove the result of Section 4.2, Note 3. Using the formulae for $\mathbf{r}_u$, $\mathbf{r}_t$ in (11) we have

$$\mathbf{r}_u \wedge \mathbf{r}_t = \lambda_u\mathbf{p} \wedge (\mathbf{c}_t + \lambda\mathbf{p}_t)$$

at the cusp point. Now $\lambda_u > 0$ (see the note on orientation in Section 3.1, and substituting for λ from (12) we find

$$\begin{aligned}\mathbf{r}_u \wedge \mathbf{r}_t &= \lambda_u\mathbf{p} \wedge \left(\mathbf{c}_t - \frac{\mathbf{c}_t.\mathbf{n}}{\mathbf{p}_t.\mathbf{n}}\mathbf{p}_t\right)\\ &= \lambda_u\mathbf{p} \wedge \frac{\mathbf{n} \wedge (\mathbf{c}_t \wedge \mathbf{p}_t)}{\mathbf{p}_t.\mathbf{n}}\\ &= \lambda_u\frac{1}{\mathbf{p}_t.\mathbf{n}}([\mathbf{p}, \mathbf{c}_t, \mathbf{p}_t]\mathbf{n} - \mathbf{p}.\mathbf{n}(\mathbf{c}_t \wedge \mathbf{p}_t))\\ &= \lambda_u\frac{1}{\mathbf{p}_t.\mathbf{n}}[\mathbf{p}, \mathbf{c}_t, \mathbf{p}_t]\mathbf{n},\end{aligned}$$

since $\mathbf{p}.\mathbf{n} = 0$. This applies for *either* choice of $\mathbf{n}$, so choosing $\mathbf{n}$ such that $[\mathbf{p}, \mathbf{c}_t, \mathbf{p}_t]/\mathbf{p}_t.\mathbf{n} > 0$ assures us that $\mathbf{n}$ is a positive multiple of $\mathbf{r}_u \wedge \mathbf{r}_t$.

12. *Second Fundamental Form*

Here, we show how to remove the apparent ambiguity in sign mentioned in Section 4.2, Note 4. Let us take axes in the tangent plane to M (at a cusp point) along $\mathbf{r}_u$, assumed here to be a positive multiple of $\mathbf{p}$ as in the note on orientation in Section 3.1, and along $\mathbf{r}_u \wedge \mathbf{n}$, where $\mathbf{n}$ is determined as in Section 4.2, Note 3. This corresponds exactly to the placing of M in Monge form, as in Section 4.2, Note 4. The ambiguity noted there amounts to an uncertainty about the sign of $\mathrm{II}(\mathbf{r}_u, \mathbf{r}_u \wedge \mathbf{n})$. Regarding $\mathbf{n}$ as a function of u, t, this is $\mathbf{n}_u.(\mathbf{r}_u \wedge \mathbf{n})$. Now

$$\mathbf{n}\,\|\mathbf{r}_u \wedge \mathbf{r}_t\| = \mathbf{r}_u \wedge \mathbf{r}_t,$$

so that, differentiating with respect to u and dotting with $\mathbf{r}_u \wedge \mathbf{r}_t$ we get

$$\mathbf{n}.(\mathbf{r}_u \wedge \mathbf{r}_t)\,\|\mathbf{r}_u \wedge \mathbf{r}_t\| = [\mathbf{r}_{uu} \wedge \mathbf{r}_t, \mathbf{r}_u, \mathbf{n}] + [\mathbf{r}_u \wedge \mathbf{r}_{uv}, \mathbf{r}_u, \mathbf{n}].$$

But the second term is zero on expansion, using $\mathbf{r}_v.\mathbf{n} = 0$ and $\mathbf{r}_{uu}.\mathbf{n} = L = 0$ (see Appendix 10). The other term is similarly equal to ME, and $E > 0$ so the sign in question is simply that of M, which is the sign of $\mathbf{p}_t.\mathbf{n}$ since $\lambda_u > 0$. Hence the sign is unambiguous.

References

Bruce, J.W. and Giblin, P.J. 1992. *Curves and Singularities*. 2nd edition, Cambridge University Press.

Cipolla, R. and Blake, A. 1992. Surface shape from deformation of apparent contours. *Int. J. of Computer Vision*, 9(2):83–112.

Cipolla, R., Åström, K.E., and Giblin, P.J. 1995. Motion from the frontier of curved surfaces. *Proc. Fifth Int. Conf. on Computer Vision*. Cambridge, Mass., pp. 269–275.

Cipolla, R., Fletcher, G.J., and Giblin, P.J. 1995. Surface geometry from cusps of apparent contours. *Proc. Fifth Int. Conf. on Computer Vision*, Cambridge, Mass., pp. 858–863.

Fletcher, G.J. and Giblin, P.J. 1996. Class based reconstruction of surfaces from singular apparent contours. *Proc. Fourth European Conf. on Computer Vision*, Cambridge, U.K., April 1996, pp. 107–116.

Giblin, P.J. and Weiss, R.S. 1987. Reconstruction of surfaces from profiles. *First Internat. Conf. on Computer Vision*, London, pp. 136–144.

Giblin, P.J. and Soares, M.G. 1988. On the geometry of a surface and its singular profiles. *Image and Vision Computing*, 6:225–234.

Giblin, P.J., Pollick, F.E., and Rycroft, J.E. 1994. Recovery of an unknown axis of rotation from the profiles of a rotating surface. *J. Opt. Soc. America*, 11A:1976–1984.

Giblin, P.J. and Weiss, R.S. 1995. Epipolar curves on surfaces. *Image and Vision Computing*, 13:33–44. Epipolar fields on surfaces.

Koenderink, J.J. 1984. What does the occluding contour tell us about solid shape? *Perception*, 13:321–330.

Koenderink, J.J. 1990. *Solid Shape*. M.I.T. Press.

Koenderink, J.J. and Van Doorn, A.J. 1982. The shape of smooth objects and the way contours end. *Perception*, 11:129–137.

O'Neill, B. 1966. *Elementary Differential Geometry*. Academic Press.

Vaillant, R. and Faugeras, O.D. 1992. Using extremal boundaries for 3D object modelling. *Patt. Recog. and Machine Intell.*, 14:157–173.